Child's Nervous System (2019) 35:1585–1590
https://doi.org/10.1007/s00381-019-04239-4

ORIGINAL ARTICLE

A three-dimensional analysis of scoliosis progression in non-idiopathic scoliosis: is it similar to adolescent idiopathic scoliosis?

Keith R. Bachmann[1] · Burt Yaszay[2,3] · Carrie E. Bartley[2] · Tracey P. Bastrom[2] · Fredrick G. Reighard[2] · Vidyadhar V. Upasani[2,3] · Peter O. Newton[2,3] · Harms Study Group Investigators

Received: 15 April 2019 / Accepted: 28 May 2019 / Published online: 10 June 2019

Abstract

Purpose To evaluate the three-dimensional (3D) characteristics of spine deformity in patients with non-idiopathic scoliosis compared with those observed in patients with adolescent idiopathic scoliosis (AIS).

Methods A retrospective chart review was conducted to identify patients with non-idiopathic scoliosis. Twenty-eight patients with neural axis (NA) abnormalities (Chiari 1, syrinx) and 20 patients with connective tissue disorder (CTD) (Marfan's, Beal's, Ehlers-Danlos syndrome, mixed) were identified. The 3D parameters of the coronal, sagittal, and axial plane were compared with 284 AIS patients with a similar range of coronal deformity.

Results The average coronal curve was similar between all three groups (AIS 48 ± 15°, CTD 43 ± 22°, and NA 49 ± 18°; $p = 0.4$). The NA patients had significantly greater 3D thoracic kyphosis (20 ± 18° vs 10 ± 15°, $p = 0.001$) and less thoracic apical vertebral rotation (− 5 ± 18° vs − 12 ± 10°, $p = 0.003$) when compared with AIS. The CTD group's 3D thoracic kyphosis ($p = 0.7$) and apical vertebral rotation ($p = 0.09$) did not significantly differ from AIS. Significant negative correlations were found in all three groups between thoracic kyphosis and coronal curve magnitude (AIS $r = -0.49$, CTD $r = -0.772$, NA $r = -0.677$, all $p < 0.001$).

Conclusions Scoliotic patients with NA abnormalities have a more kyphotic, less-rotated 3D profile than patients with AIS, while scoliosis patients with CTD have 3D features similar to AIS. Irrespective of the underlying diagnosis, however, greater scoliotic curves were associated with a greater loss of intersegmental kyphosis, suggesting a similar biomechanical pathophysiology for curve progression.

Keywords Scoliosis · Syndromic scoliosis · Adolescent idiopathic scoliosis, 3D, deformity

Introduction

Prior work has shown that adolescent idiopathic scoliosis (AIS) is associated with hypokyphosis in the thoracic spine [1–5] and that the sagittal deformity is under represented on plain radiography [6, 7]. The literature is sparse, however, in defining the three-dimensional (3D) deformity of ambulatory patients with syndromic scoliosis and scoliosis associated with connective tissues disorders. Glard and colleagues examined the sagittal and axial plane of patients with Marfan's syndrome and found that apical axial rotation significantly correlated with the coronal curve [8] and that segmental extension, or lordosis, was found at the thoracic apex in approximately 80% of patients [9]. The two-dimensional (2D) description of syndromes as a result of connective tissue disorders has focused on kyphoscoliotic deformities [10–14] while the sagittal profile in syringomyelia is noted to be hyperkyphotic in 2D [15–21].

It remains unclear whether the imbalance of spinal growth with resultant hypokyphosis is a primary mechanism for column buckling or whether the continued anterior overgrowth is due to the Hueter-Volkmann principle after the spinal column

This study was conducted at Rady Children's Hospital, San Diego, CA.

✉ Burt Yaszay
byaszay.rady@gmail.com

[1] Department of Orthopedics, University of Virginia Medical Center, Charlottesville, VA, USA

[2] Department of Orthopedics, Rady Children's Hospital, 3030 Children's Way, MC5062, San Diego, CA 92123, USA

[3] Department of Orthopedics, University of California, San Diego, CA, USA

buckles out of plane. Examining the sagittal plane in syndromic scoliosis with various curve sizes may help to shed light on the influence of anterior overgrowth versus mechanical effects leading to hypokyphosis. Thus, the purpose of the current study was to examine the three-dimensional deformity associated with syndromic scoliosis compared with idiopathic scoliosis. Also of interest was the relationship of the true sagittal deformity as it relates to the severity of the coronal curve magnitude.

Materials and methods

Institutional review board approval was obtained for this single-center, retrospective chart and radiographic review. Medical records and group billing records were queried to find patients treated for scoliosis that also had a diagnosis of a syndrome (Marfan's, Beal's, Ehlers-Danlos, Syringomyelia, Chiari 1 malformation). A total of 272 patients were found with the medical record and 176 with the billing records. There were 55 patients who came up on both search queries leaving 393 unique patients. The individual charts were then reviewed to determine the secondary diagnoses and determine the magnitude of spinal curvature. The inclusion criteria included one of the diagnoses of interest, a curve > 20°, age 10 ≤ 19 years, and synchronized, upright, biplanar spine radiographs with the EOS imaging system (EOS Imaging, Paris, France). Patients were excluded if they had undergone operations prior to the inclusion dates, any neuromuscular scoliosis including spina bifida, cerebral palsy, polio, congenital scoliosis, paralytic scoliosis, or images that were not obtained with the EOS imaging unit. Of the 393 patients, 48 met the inclusion criteria: 20 with a connective tissue disorder (CTD) and 28 with a neural axis disorder (NA). A cohort of 284 AIS patients who had EOS images were then matched to the other groups based on distribution of curve sizes.

All patients' images were loaded into SterEOS software for 3D spinal reconstruction from T1 to L5. The 3D reconstructions were subsequently exported to MATLAB for further analysis. Previous work has shown these 3D reconstructions to be accurate to within 1° of CT imaging for coronal Cobb angle and thoracic kyphosis [22]. 3D measurements were made utilizing local vertebral reference planes in order to minimize distortional effects of rotation as previously described [7]. Such measurements allow for effective measurement of sagittal deformity in its plane of origin by measuring the sagittal kyphosis of each vertebra and disc individually, at zero degrees of axial rotation, and subsequently summing these measurements over a region of interest [7]. Kyhosis is represented as a positive value, lordosis a negative value.

The following were compared between the AIS, CTD, and NA groups: sex, 2D coronal curve magnitude, pelvic parameters, 3D axial rotation, and 3D local-summed plane measurements for sagittal and coronal curves. For continuous variables, ANOVA with the Bonferroni post hoc comparisons was utilized. Pearson correlation coefficient was utilized to evaluate the relationship between coronal curve severity and 3D local-summed measurement of T5–T12 sagittal kyphosis. Analyses were performed utilizing SPSS v. 12 (SPSS Inc., Chicago, IL) and alpha was set at $p < 0.05$ to declare significance.

Results

There was a significant difference in the distribution of sex across the three groups, with the AIS cohort having the lowest percentage of male patients (16%), followed by NA (28%), and CTD (45%), ($p = 0.002$). The 2D major coronal curve was similar between the three groups: AIS 48 ± 15°, CTD 43 ± 22°, and NA 49 ± 18° ($p = 0.41$). Significant differences between the AIS and CTD groups were found in pelvic incidence (52 ± 12° AIS, 46 ± 14° CTD, $p = 0.023$) and sacral slope (44 ± 9° AIS, 38 ± 13° CTD, $p = 0.013$) (Table 1).

No differences were observed between the CTD and AIS groups in terms of apical axial rotation of the proximal thoracic, thoracic, or thoracolumbar/lumbar curves. The NA disorders group had significantly less rotation in all three curves compared with the AIS group and less rotation than the CTD group in the proximal thoracic and thoracolumbar/lumbar regions (Table 1).

The NA group was found to have significantly more 3D T5-T12 kyphosis (20 ± 18°) than the AIS cohort (10 ± 15°)($p = 0.001$). The CTD group's 3D T5-T12 kyphosis was not significantly different than the other two groups' (11 ± 20°, $p > 0.1$). The CTD group was significantly less kyphotic from T10-L2 than the AIS group (− 0.3° vs − 6°, $p = 0.048$). No significant differences were observed between any of the groups in T1–T5 kyphosis ($p = 0.8$) or T12-S1 lordosis ($p = 0.09$) (Table 1). In all three groups, greater coronal curve severity was associated with less 3D thoracic kyphosis (AIS, $r = -0.49$; CTD, $r = -0.77$; NA, $r = -0$. (Fig. 1). An example from each group of the 3D reconstructions and the 3D sagittal profile can be found in Figs. 2, 3, and 4.

Discussion

Three-dimensional analysis revealed significantly different sagittal profiles for patients with syndromic scoliosis compared with those with AIS. The patients with connective tissue disorders were found to have a sagittal and rotational profile mostly similar to the idiopathic cohort, but with less pelvic incidence and more kyphosis through the T10-L2 segment. The thoracic kyphosis was similar to AIS. It may be possible that in the connective tissue group, having less kyphosis is

Table 1 3D apical rotation, 3D sagittal alignment, and pelvic parameter comparisons between groups

		AIS	NA	CTD	*p* value	AIS vs. NA	AIS vs. CTD	NA vs CTD
3D apical rotation	Prox. Thorocic	7 ± 6°	1 ± 8°	7 ± 6°	< 0.001	**< 0.001**	0.99	**0.002**
	Thoracic	− 12 ± 10°	− 5 ± 18°	− 7 ± 12°	< 0.001	**0.003**	0.92	0.99
	Lumbar	8 ± 9°	3 ± 11°	11 ± 16°	0.023	**0.047**	0.96	**0.038**
3D sagittal	T1-T5	17 ± 8°	17 ± 6°	18 ± 14°	0.819			
	T5-T12	10 ± 15°	20 ± 18°	11 ± 20°	< 0.004	**0.001**	0.754	0.125
	T10-L2	− 6 ± 12°	− 1 ± 15°	− 0.3 ± 12°	0.03	0.055	**0.048**	0.99
	T12-S1	− 60 ± 13°	− 63 ± 15°	− 55 ± 17°	0.093			
Pelvic parameters	Pelvic Incidence	52 ± 12°	48 ± 12°	46 ± 14°	0.03	0.12	**0.023**	0.99
	Sacral Slope	44 ± 9°	44 ± 10°	38 ± 13°	0.017	0.668	**0.013**	0.147
	Pelvic Tilt	8 ± 8°	5 ± 9°	7 ± 9°	0.18			

Bold values represent statistical significance

most compatible with the lower pelvic incidence so as to create a more balanced transition between the lumbar and thoracic regions of the spine.

The kyphosis in patients with neural axis associated scoliosis was found to be greater than that observed in the AIS group. Ouellet et al. [17] and Loder et al. [16] also reported increased thoracic kyphosis measured in 2D for patients with syringomyelia versus those without. In the current study, the thoracic kyphosis was measured in 3D by summing the kyphosis at each level between T5 and T12 to account for the distortion that is created by rotation and translation that is observed on 2D images [7, 23]. While the average kyphosis in the neural axis patients was higher than that seen in the AIS patients, it was still within the normal range described by the Lenke classification [24]. Although that classification only applies to AIS, it is important to understand how the syndromic patients' curve characteristics deviate from idiopathic scoliosis as this information may help to distinguish which patients might need an MRI, particularly in the presence of hyperkyphosis [20].

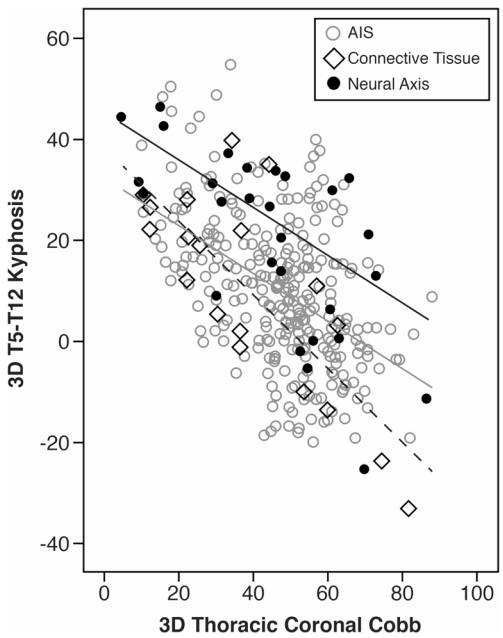

Fig. 1 Scatterplot of correlation between 3D Cobb and Kyphosis. Trendline for AIS is represented in solid gray line, connective tissue is dotted black line, and neural axis is solid black line. All 3 correlations were statistically significant ($p < 0.001$)

Apical rotation was also significantly less in the neural axis group compared with AIS, suggesting that these diagnoses may have different mechanisms that cause the spinal column to buckle out of plane. The neural axis population demonstrated a more pure coronal deviation than the sagittal flattening and axial rotation seen in AIS.

One commonality between the three groups was that greater coronal curve magnitudes were associated with less 3D thoracic kyphosis. The benefit of the 3D analysis is that the observed kyphosis is not due to rotational abnormality. As such, we speculate there may be a similar pathway of progression that involves the spinal column buckling out of plane, which results in an unloading of the spinal column in both the anterior and convex directions that contributes to disproportionate growth via the Hueter-Volkmann law, all of which feeds the "vicious cycle" of progression discussed by Stokes et al. [25].

Limitations to the current study include its retrospective nature. Additionally, this was a cross-sectional analysis which helps to address differences in the sagittal and axial profiles between diagnoses; however, the conclusions regarding progression are limited as serial data was not available to evaluate progression within the same patients over time. It is clear that there is an association between curve severity and kyphosis; however, further study would benefit from the addition of longitudinal data.

In conclusion, curves associated with connective tissue disorders seem to closely mimic those of adolescent idiopathic scoliosis in three dimensions, while neural axis disorders

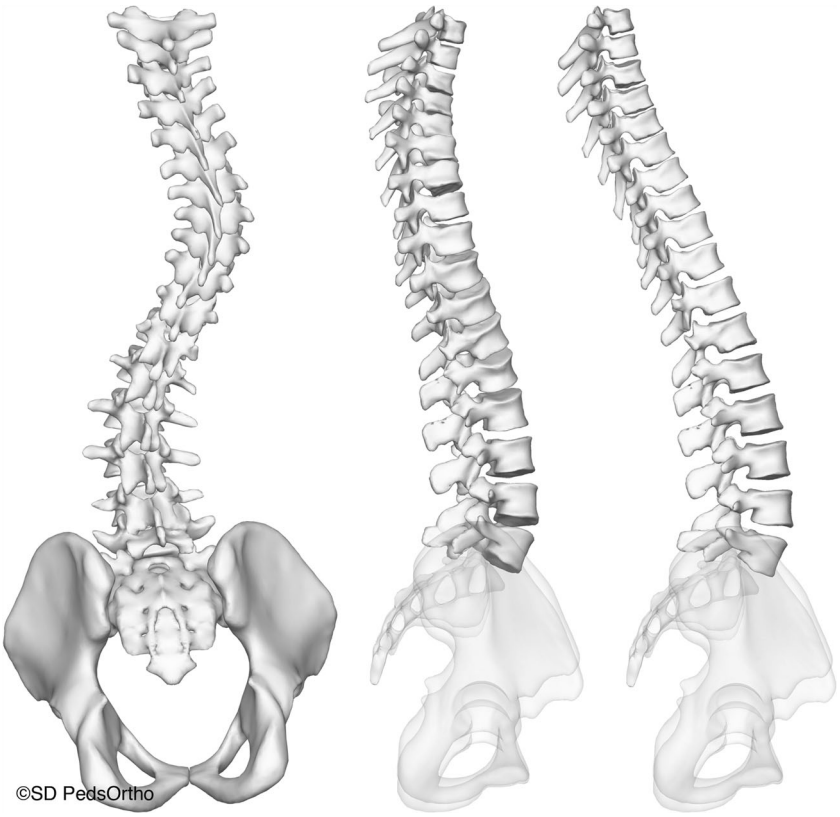

Fig. 2 3D models of the spine of a patient with neural axis-associated scoliosis. The figure includes the PA view (left), lateral view without adjustment for axial rotation (center), and the 3D lateral view after removal of the axial plane deformity (right)

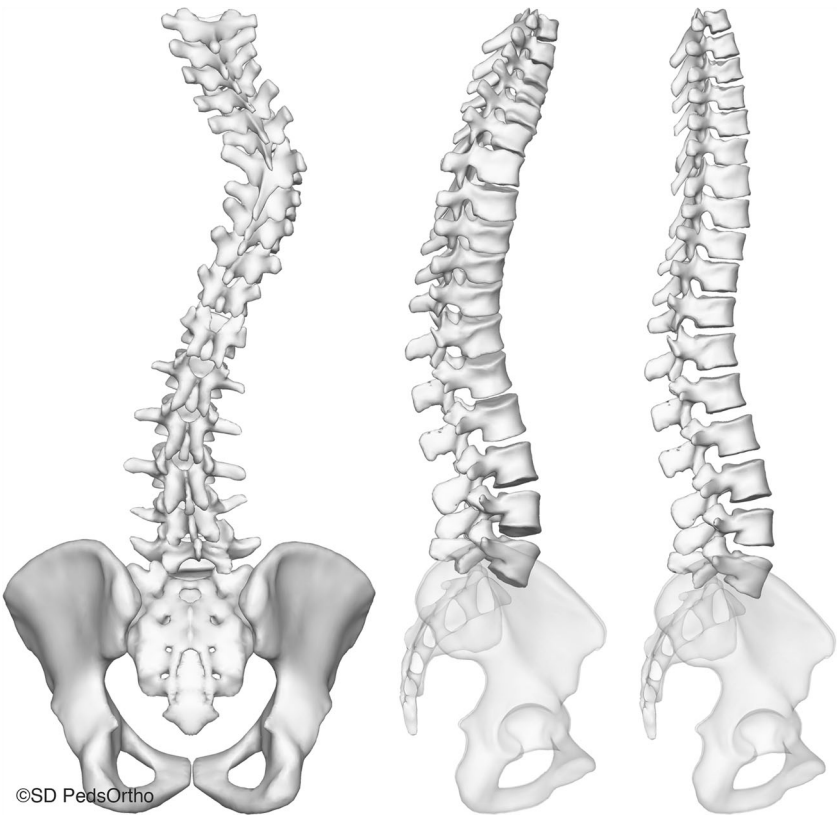

Fig. 3 3D models of the spine of a patient with scoliosis associated with a connective tissue disorder. Lateral view without adjustment for axial rotation (center), and the 3D lateral view after removal of the axial plane deformity (right)

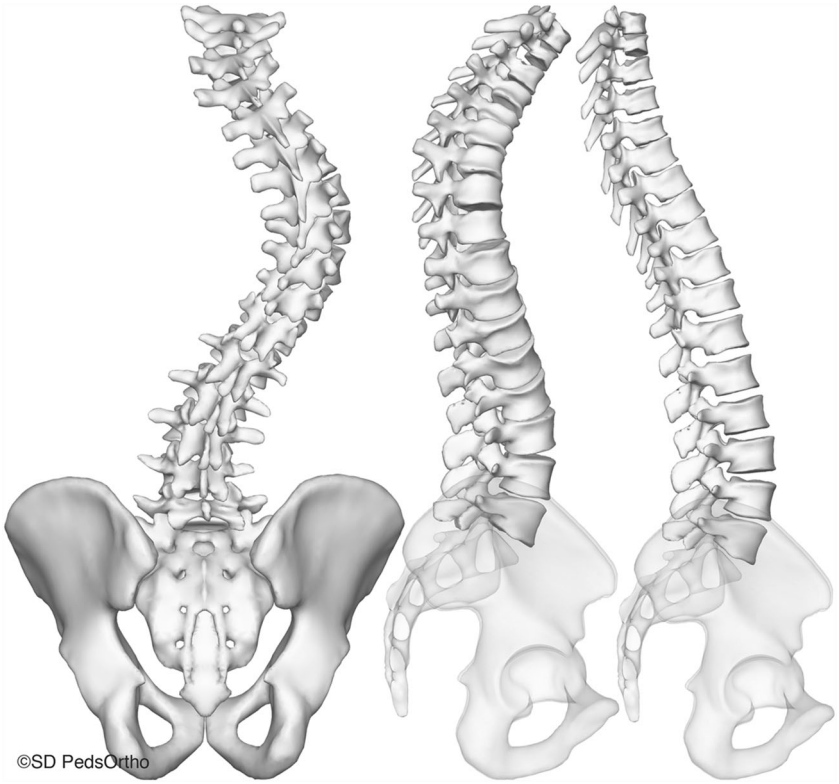

Fig. 4 3D models of the spine of a patient with adolescent idiopathic scoliosis. The figure includes the PA view (left), lateral view without adjustment for axial rotation (center), and the 3D lateral view after removal of the axial plane deformity (right)

demonstrate greater kyphosis in the sagittal plane and less rotation in the axial plane. In this snapshot, the etiology and three-dimensional deformity differed between groups. However, with greater coronal deformity there was less thoracic kyphosis to frank lordosis. Irrespective of the underlying diagnosis, larger scoliotic curves had less intersegmental kyphosis, suggesting a similar biomechanical pathophysiology for curve progression.

Acknowledgements Harms Study Group Investigators:
Aaron Buckland, MD; New York University
Amer Samdani, MD; Shriners Hospitals for Children—Philadelphia
Amit Jain, MD; Johns Hopkins Hospital
Baron Lonner, MD; Mount Sinai Hospital
Benjamin Roye, MD; Columbia University
Burt Yaszay, MD; Rady Children's Hospital
Chris Reilly, MD; BC Children's Hospital
Daniel Hedequist, MD; Boston Children's Hospital
Daniel Sucato, MD; Texas Scottish Rite Hospital
David Clements, MD; Cooper Bone & Joint Institute New Jersey
Firoz Miyanji, MD; BC Children's Hospital
Harry Shufflebarger, MD; Nicklaus Children's Hospital
Jack Flynn, MD; Children's Hospital of Philadelphia
Jahangir Asghar, MD; Cantor Spine Institute
Jean Marc Mac Thiong, MD; CHU Sainte-Justine
Joshua Pahys, MD; Shriners Hospitals for Children—Philadelphia
Juergen Harms, MD; Klinikum Karlsbad-Langensteinbach, Karlsbad
Keith Bachmann, MD; University of Virginia
Larry Lenke, MD; Columbia University
Mark Abel, MD; University of Virginia
Michael Glotzbecker, MD; Boston Children's Hospital
Michael Kelly, MD; Washington University
Michael Vitale, MD; Columbia University
Michelle Marks, PT, MA; Setting Scoliosis Straight Foundation
Munish Gupta, MD; Washington University
Nicholas Fletcher, MD; Emory University
Patrick Cahill, MD; Children's Hospital of Philadelphia
Paul Sponseller, MD; Johns Hopkins Hospital
Peter Gabos, MD: Nemours/Alfred I. duPont Hospital for Children
Peter Newton, MD; Rady Children's Hospital
Peter Sturm, MD; Cincinnati Children's Hospital
Randal Betz, MD; Institute for Spine & Scoliosis
Ron Lehman, MD; Columbia University
Stefan Parent, MD: CHU Sainte-Justine
Stephen George, MD; Nicklaus Children's Hospital
Steven Hwang, MD; Shriners Hospitals for Children—Philadelphia
Suken Shah, MD; Nemours/Alfred I. duPont Hospital for Children
Tom Errico, MD; Nicklaus Children's Hospital
Vidyadhar Upasani, MD; Rady Children's Hospital

Funding information Research support is gratefully acknowledged from the Rady Children's Foundation Assaraf Family Research Fund and from funding to the Setting Scoliosis Straight Foundation from DePuy Synthes Spine, EOS imaging, K2M, Medtronic, NuVasive and Zimmer Biomet in support of Harms Study Group Research.

Compliance with ethical standards

Conflict of interest Dr. Bachmann reports funding to his institution from Setting Scoliosis Straight, during the conduct of this study; personal fees from Nuvasive, outside the submitted work.

Dr. Yaszay reports grants to his institution from the Setting Scoliosis Straight Foundation, during the conduct of the study; grants and personal fees from K2M, grants and personal fees from DePuy Synthes Spine, grants and personal fees from Nuvasive, personal fees from Medtronic,

grants and personal fees from Orthopediatrics, personal fees from Stryker, personal fees from Globus, grants from Setting Scoliosis Straight Foundation, personal fees from Biogen, outside the submitted work. In addition, Dr. Yaszay has a patent K2M with royalties paid.

Dr. Upasani reports grants to his institution from the Setting Scoliosis Straight Foundation, during the conduct of this study; personal fees from DePuy Synthes Spine, personal fees from OrthoPediatrics, outside the submitted work.

Dr. Newton reports grants to his institution from the Setting Scoliosis Straight Foundation (SSSF receives grants from from DePuy Synthes Spine, EOS imaging, K2M, Medtronic, NuVasive and Zimmer Biomet in support of Harms Study Group research), during the conduct of the study; grants and other from the Setting Scoliosis Straight Foundation, other from the Rady Children's Specialists, grants, personal fees and non-financial support from the DePuy Synthes Spine, grants and other from SRS, grants from EOS imaging, personal fees from Thieme Publishing, grants from NuVasive, other from Electrocore, personal fees from Cubist, other from International Pediatric Orthopedic Think Tank, grants, non-financial support and other from Orthopediatrics, grants, personal fees and non-financial support from K2M, grants and non-financial support from Alphatech, grants from Mazor Robotics, outside the submitted work; In addition, Dr. Newton has a patent Anchoring systems and methods for correcting spinal deformities (8540754) with royalties paid to DePuy Synthes Spine, a patent Low profile spinal tethering systems (8123749) licensed to DePuy Spine, Inc., a patent Screw placement guide (7981117) licensed to DePuy Spine, Inc., a patent compressor for use in minimally invasive surgery (7189244) licensed to DePuy Spine, Inc., and a patent posterior spinal fixation pending to K2M.

All remaining authors report funding to their institutions from the Setting Scoliosis Straight Foundation, during the conduct of this study; no other conflicts of interest, outside the submitted work.

References

1. Deacon P, Archer IA, Dickson RA (1987) The anatomy of spinal deformity: a biomechanical analysis. Orthopedics 10(6):897–903
2. Deacon P, Flood BM, Dickson RA (1984) Idiopathic scoliosis in three dimensions. A radiographic and morphometric analysis. J Bone Joint Surg Br 66(4):509–512
3. Dickson RA, Lawton JO, Archer IA, Butt WP (1984) The pathogenesis of idiopathic scoliosis. Biplanar spinal asymmetry. J Bone Joint Surg Br 66(1):8–15
4. Millner PA, Dickson RA (1996) Idiopathic scoliosis: biomechanics and biology. Eur Spine J 5(6):362–373
5. Roaf R (1966) The basic anatomy of scoliosis. J Bone Joint Surg Br 48(4):786–792
6. Hayashi K, Upasani VV, Pawelek JB, Aubin CE, Labelle H, Lenke LG, Jackson R, Newton PO (2009) Three-dimensional analysis of thoracic apical sagittal alignment in adolescent idiopathic scoliosis. Spine (Phila Pa 1976) 34(8):792–797. https://doi.org/10.1097/BRS.0b013e31818e2c36
7. Newton PO, Fujimori T, Doan J, Reighard FG, Bastrom TP, Misaghi A (2015) Defining the "three-dimensional sagittal plane" in thoracic adolescent idiopathic scoliosis. J Bone Joint Surg Am 97(20):1694–1701. https://doi.org/10.2106/JBJS.O.00148
8. Glard Y, Pomero V, Collignon P, Skalli W, Jouve JL, Bollini G (2009) Three-dimensional analysis of the vertebral rotation associated with the lateral deviation in Marfan syndrome spinal deformity. J Pediatr Orthop B 18(1):51–56. https://doi.org/10.1097/BPB.0b013e3283153fd5
9. Glard Y, Pomero V, Collignon P, Skalli W, Jouve JL, Bollini G (2008) Sagittal balance in scoliosis associated with Marfan syndrome: a stereoradiographic three-dimensional analysis. J Child Orthop 2(2):113–118. https://doi.org/10.1007/s11832-008-0083-3
10. Birch JG, Herring JA (1987) Spinal deformity in Marfan syndrome. J Pediatr Orthop 7(5):546–552
11. Garreau de Loubresse C, Mullins MM, Moura B, Marmorat JL, Piriou P, Judet T (2006) Spinal and pelvic parameters in Marfan's syndrome and their relevance to surgical planning. J Bone Joint Surg Br 88(4):515–519. https://doi.org/10.1302/0301-620x.88b4.17034
12. McMaster MJ (1994) Spinal deformity in Ehlers-Danlos syndrome. Five patients treated by spinal fusion. J Bone Joint Surg Br 76(5):773–777
13. Rabenhorst BM, Garg S, Herring JA (2012) Posterior spinal fusion in patients with Ehlers-Danlos syndrome: a report of six cases. J Child Orthop 6(2):131–136. https://doi.org/10.1007/s11832-012-0393-3
14. Sponseller PD, Hobbs W, Riley LH 3rd, Pyeritz RE (1995) The thoracolumbar spine in Marfan syndrome. J Bone Joint Surg Am 77(6):867–876
15. Arai S, Ohtsuka Y, Moriya H, Kitahara H, Minami S (1993) Scoliosis associated with syringomyelia. Spine (Phila Pa 1976) 18(12):1591–1592
16. Loder RT, Stasikelis P, Farley FA (2002) Sagittal profiles of the spine in scoliosis associated with an Arnold-Chiari malformation with or without syringomyelia. J Pediatr Orthop 22(4):483–491
17. Ouellet JA, LaPlaza J, Erickson MA, Birch JG, Burke S, Browne R (2003) Sagittal plane deformity in the thoracic spine: a clue to the presence of syringomyelia as a cause of scoliosis. Spine (Phila Pa 1976) 28(18):2147–2151. https://doi.org/10.1097/01.BRS.0000091831.50507.46
18. Ozerdemoglu RA, Denis F, Transfeldt EE (2003) Scoliosis associated with syringomyelia: clinical and radiologic correlation. Spine (Phila Pa 1976) 28(13):1410–1417. https://doi.org/10.1097/01.BRS.0000067117.07325.86
19. Qiu Y, Zhu Z, Wang B, Yu Y, Qian B, Zhu F (2008) Radiological presentations in relation to curve severity in scoliosis associated with syringomyelia. J Pediatr Orthop 28(1):128–133. https://doi.org/10.1097/bpo.0b013e31815ff371
20. Spiegel DA, Flynn JM, Stasikelis PJ, Dormans JP, Drummond DS, Gabriel KR, Loder RT (2003) Scoliotic curve patterns in patients with Chiari I malformation and/or syringomyelia. Spine (Phila Pa 1976) 28(18):2139–2146. https://doi.org/10.1097/01.BRS.0000084642.35146.EC
21. Whitaker C, Schoenecker PL, Lenke LG (2003) Hyperkyphosis as an indicator of syringomyelia in idiopathic scoliosis: a case report. Spine (Phila Pa 1976) 28(1):E16–E20. https://doi.org/10.1097/01.brs.0000038240.88287.0b
22. Glaser DA, Doan J, Newton PO (2012) Comparison of 3-dimensional spinal reconstruction accuracy: biplanar radiographs with EOS versus computed tomography. Spine (Phila Pa 1976) 37(16):1391–1397. https://doi.org/10.1097/BRS.0b013e3182518a15
23. Stagnara P (1968) Medical observation and tests for scoliosis. Rev Lyon Med 17(9):391–401
24. Lenke LG, Edwards CC 2nd, Bridwell KH (2003) The Lenke classification of adolescent idiopathic scoliosis: how it organizes curve patterns as a template to perform selective fusions of the spine. Spine (Phila Pa 1976) 28(20):S199–S207. https://doi.org/10.1097/01.BRS.0000092216.16155.33
25. Stokes IA, Spence H, Aronsson DD, Kilmer N (1996) Mechanical modulation of vertebral body growth. Implications for scoliosis progression. Spine (Phila Pa 1976) 21(10):1162–1167